THE ASTROPHYSICAL JOURNAL, 422:L13–L16, 1994 February 10

NEUTRAL HYDROGEN ABSORPTION IN NGC 1068 AND NGC 3079

J. F. GALLIMORE,[1] S. A. BAUM, AND C. P. O'DEA
Space Telescope Science Institute, 3700 San Martin Drive, Baltimore, MD 21218

E. BRINKS
NRAO, P.O. Box O, Socorro, NM 87801-0387

AND

A. PEDLAR
NRAL, Jodrell Bank, Macclesfield, Cheshire SK11 9DL, UK

Received 1993 October 4; accepted 1993 November 18

ABSTRACT

We have used the VLA in A configuration to obtain spatially resolved 21 cm absorption spectra of NGC 1068 and NGC 3079. The bulk of the absorbing H I in NGC 1068 appears to be located in the inner disk and is oriented such that the brighter, northeast radio lobe is located in front of the disk and the fainter, southwest radio lobe is located behind. We find evidence for a shock front inside the leading edge of the stellar bar based on the kinematics and column density distribution of the H I. Near the radio nucleus of NGC 1068 the H I appears to be participating in a wind-driven outflow. In NGC 3079 we detect slightly resolved H I absorption against the radio core. This absorption is characterized by strong, multiple components: (1) broad absorption (FWZI $\gtrsim$ 895 km s^{-1}) with a deep core near the systemic velocity and a slight blue asymmetry, and (2) red- and blueshifted components which are slightly resolved by the VLA beam. These Doppler-shifted components might arise in a wind-driven outflow or a slightly resolved circumnuclear ring ($\sim$90 pc radius). Assuming circular orbits, the virial mass interior to the alleged ring would exceed 10^8 $M_\odot$.

Subject headings: galaxies: individual (NGC 1068, NGC 3079) — galaxies: ISM — galaxies: kinematics and dynamics — galaxies: Seyfert — radio lines: galaxies

1. INTRODUCTION

We have begun a program of high angular resolution, aperture synthesis observations of 21 cm H I absorption in radio-bright Seyfert galaxies. The aim of this project is to map the distribution and kinematics of the circumnuclear H I on arcsecond-subarcsecond scales. These observations of the *cold* circumnuclear interstellar medium (ISM) in Seyfert galaxies complement optical emission-line observations which show only the ISM which has been shocked or illuminated by the active galactic nucleus (AGN). With the H I data we hope to develop a more complete picture of the fueling and exhaust mechanisms of AGNs.

Using the VLA[2] in A configuration, we have obtained 21 cm absorption spectra of 12 Seyfert galaxies with bright, extended radio continuum emission at 1″–2″ resolution. We report here the preliminary results for NGC 1069 and NGC 3079.

2. OBSERVATIONS AND DATA REDUCTION

The data were taken with the VLA in A configuration using the 4IF mode. All of the data reduction and calibration was performed using standard procedures within AIPS (Gallimore et al. 1994). The data presented in this *Letter* were extracted from naturally weighted, continuum-subtracted, and CLEANed channel maps. These maps span a bandwidth of 998 km s^{-1} with a velocity resolution of 20.8 km s^{-1}. The restoring beam size (FWHM) for NGC 1068 is 2″.1 × 1″.5 (P.A. −24°.4) and for NGC 3079 is 1″.7 × 1″.6 (P.A. 19°.9). The rms noise for NGC 1068 (NGC 3079) is $\sim$0.6 (0.5) mJy beam^{-1} channel^{-1}, comparable to the expected thermal noise.

3. RESULTS

3.1. H I *Absorption in NGC 1068*

NGC 1068 is a type 2 Seyfert galaxy with a hidden broad-line region (Antonucci & Miller 1985). A schematic of the inner 40″ of NGC 1068 is provided in Figure 1. The radio continuum emission from this galaxy is dominated by a 13″ radio triple extending southwest to northeast. The central radio source is the apex for an optical emission-line "cone" (Evans et al. 1991; Pogge 1988) and the center of a 30″ stellar bar (Thronson et al. 1989), each of which is roughly aligned with the extended radio structure. At the core of the nucleus is a 1″ radio triple (Ulvestad, Neff, & Wilson 1987) which is slightly resolved in our observations. A ring of bright, clumpy CO emission encircles the 13″ radio structure and 30″ stellar bar (Kaneko et al. 1992a; Planesas, Scoville, & Myers 1991). Interior to the CO ring is an inner disk of bright optical continuum and line emission (Bland-Hawthorn, Sokolowski, & Cecil 1991; Sandage 1961). The inner disk appears to be nearly face-on, with inclination $i \sim 30°$–$40°$ based on the shape of the optical isophotes (Kaneko et al. 1989; Hodge 1968) and the large-scale H I emission (Brinks et al. 1994). We adopt $v_{sys} \simeq 1140$ km s^{-1} (Heckman, Balick, & Sullivan 1978), corresponding to a distance of 22.8 Mpc ($H_0 = 50$ km s^{-1} Mpc^{-1}). The projected scale is 111 pc arcsec^{-1}.

We have detected H I absorption over the entire southwest radio lobe and the southern half of the radio core of NGC

[1] Also Astronomy Department, University of Maryland, College Park, MD 20742.

[2] The Very Large Array is a facility of the National Radio Astronomy Observatory, which is operated by Associated Universities, Inc., under Cooperative agreement with the National Science Foundation.

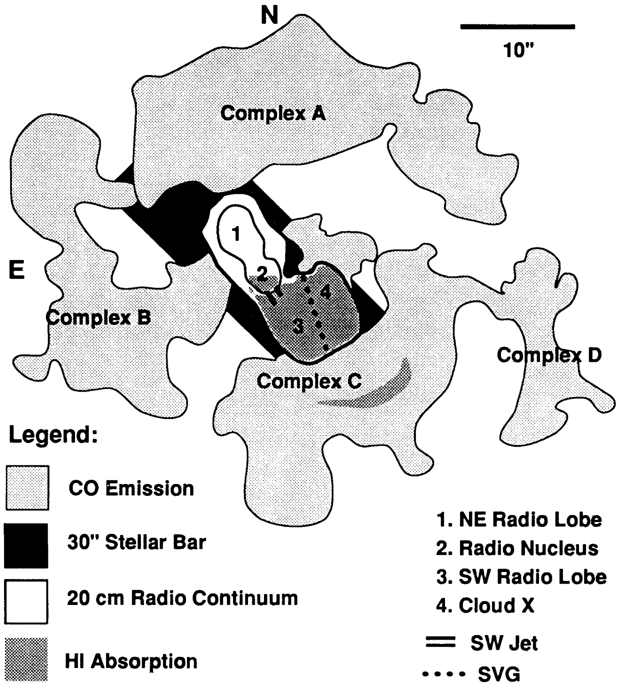

FIG. 1.—Schematic of the inner 40″ of NGC 1068. Regions of bright 20 cm radio continuum emission, bright CO ($J = 1$–0) emission (labeled as complexes A–D after Kaneko et al. 1992a), H I absorption, and the stellar bar (after Thronson et al. 1989) are shaded with contrasting gray levels as shown in the legend on the figure. For clarity, the ring of faint radio continuum which coincides with the CO ring is not indicated on this schematic. The steep velocity gradient (SVG) is marked by a dotted line, and the southwest "jet" is outlined by black, parallel bars just southwest of the radio core. The horizontal-scale bar represents 10″.

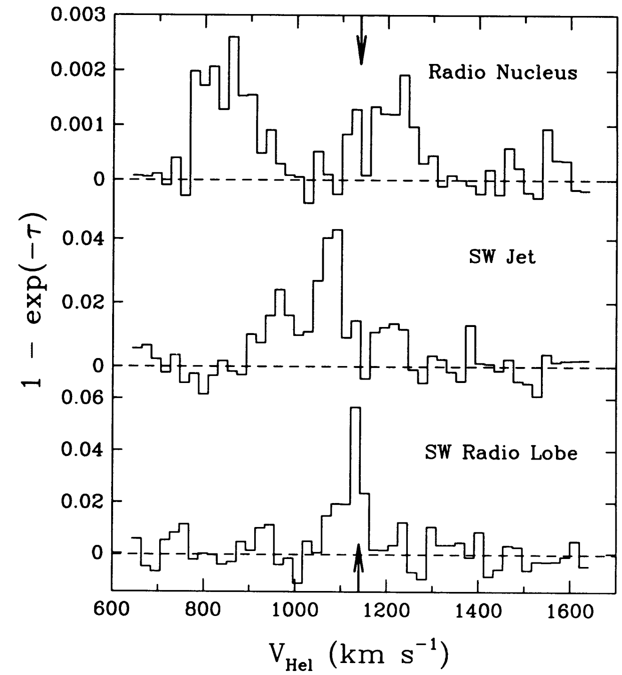

FIG. 2.—Continuum-weighted optical depth spectra for NGC 1068. The spectra, in order from top to bottom, were extracted from (1) a 1″ square region centered 0″.7 southeast of the radio core, (2) a 1″ square region covering the southwest jet, and and (3) a 2″.5 square region in the southwest radio lobe centered 8″ south and 2″ west of the radio core. The systemic velocity (1140 km s^{-1}) is indicated by vertical arrows. Following extraction, weak linear baselines were subtracted from the radio core and southwest jet spectra. A strongly aberrant value at 1360 km s^{-1} in the radio core spectrum was clipped to better scale the spectrum.

1068. There is also weak H I absorption associated with a clump of bright CO and weak radio continuum emission $\sim 15''$ southwest of the radio core (complex C after Kaneko et al. 1992a). Three kinematically distinct regions are apparent in the absorption maps of NGC 1068: (1) a portion of the inner disk which is seen in absorption against the extended southwest radio lobe, (2) rapid outflow coincident with the linear radio structure extending 1″–3″ southwest of the nucleus (the southwest "jet"), and (3) broad, double absorption lines located over the southern half of the bright, slightly resolved radio core. We extracted continuum-weighted optical depth spectra (e.g., Dickey, Brinks, & Puche 1992) from the radio core, southwest jet, and southwest lobe regions (Fig. 2). In Figure 3 we present maps of the H I column densities and velocity centers based on Gaussian fits to the line profiles over the southwest radio lobe and complex C. For 21 cm absorption the H I column density is given by $N_{\rm H\,I} = CT_{\rm spin} \int \tau(v)dv$, where $C = 1.83 \times 10^{18}$ cm^{-2} K^{-1} (km s^{-1})$^{-1}$, $\tau(v)$ is the optical depth at velocity v, and $T_{\rm spin}$ is the spin temperature (assumed to be 100 K in Fig. 3).

3.1.1. *The Inner Disk: Evidence for a Bar-induced Shock Front*

The absorption-line profiles over the southwest radio lobe and complex C have line widths (FWHM) $\lesssim 40$ km s^{-1}, and the velocity map is broadly consistent with rotation leading toward the northwest. This velocity pattern is comparable to that seen in optical emission lines (e.g., Kaneko et al. 1992b), so the absorbing H I probably resides in the inner disk. H I clouds likely occupy the entire inner disk, but we are able to detect only the fraction of the disk which is seen in absorption against the southwest radio lobe. That no H I absorption is detected over the northeast radio lobe indicates that it must be located on the near side of the inner disk (i.e., the northeast lobe is pointed toward us), and the fainter, southwest radio lobe is located on the far side of the inner disk. This jet/disk orientation is consistent with (1) cylindrical outflow models (e.g., Unger et al. 1992; Cecil, Bland, & Tully 1990, hereafter CBT), (2) the extinction of [O III] emission southwest of the nucleus (Unger et al. 1992; Evans et al. 1991), and (3) the depolarization of radio continuum emission from the southwest radio lobe (cf. Wilson & Ulvestad 1987).

The moment maps (Fig. 3) reveal structure that cannot, however, be explained by simple galaxian rotation. Most noticeably there is a steep velocity gradient (SVG) with isovelocity contours running north-south through the center of the southwest radio lobe (labeled "SVG" on Figs. 1 and 3). Leading the SVG is a region of enhanced optical depth ("Cloud X" on Figs. 1 and 3). The leading edge of Cloud X coincides with a patch of weak CO emission (Kaneko et al. 1992a), so the jump in τ likely reflects a true enhancement in $N_{\rm H\,I}$ rather than a drop in the local $T_{\rm spin}$. We note that the SVG and Cloud X are located just inside the leading edge of the 30″ stellar bar (cf. Thronson et al. 1989, Fig. 5*a*) suggesting that the SVG is a shock front in the stellar bar. Such shock fronts and leading density enhancements have appeared in numerical simulations of gas flows in bar potentials (Athanassoula 1992a, b and references therein).

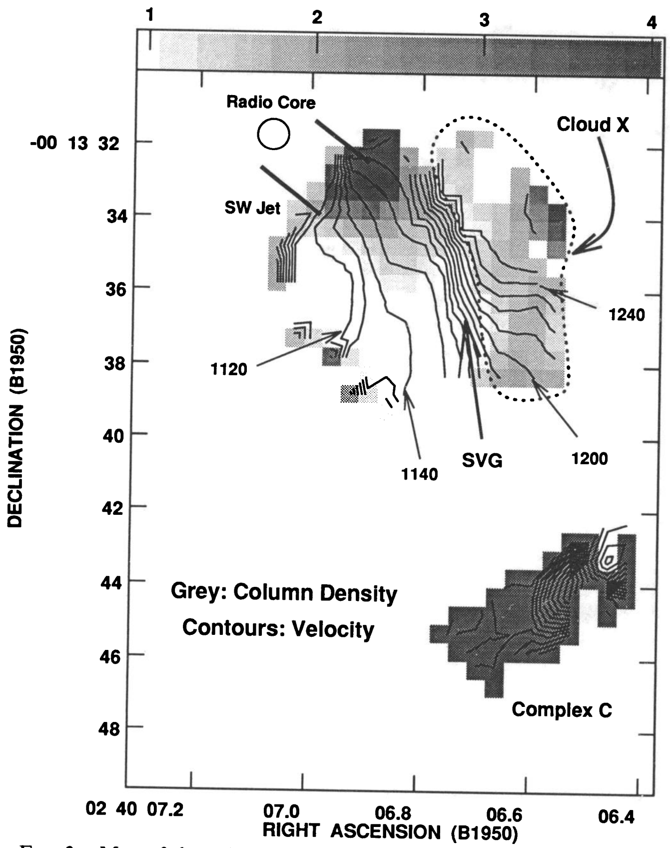

FIG. 3.—Map of the column densities (gray scale) and centroid velocities (*contours*) of absorption lines covering the southwest radio lobe and complex C in NGC 1068. The display range for the column density map is (1–4) $\times 10^{21}$ ($T_{\rm spin}$/100 K) cm^{-2}. Velocity contours are presented at 10 km s^{-1} intervals, and select contours are labeled in units (km s^{-1}). "Cloud X" (see text) is outlined by a dotted line, and other features relevant to the text are labeled.

3.1.2. *Outflow and Streaming at the Southwest Jet*

The H I absorption profile at the southwest jet (Fig. 2) is composed of two blended, blueshifted lines and a much weaker redshifted component. From a Gaussian decomposition, the velocity centers of the blueshifted lines are located at -176 ± 7 and -65 ± 3 km s^{-1} relative to $v_{\rm sys}$. The optical depth of the stronger line is comparable to that found in the inner disk (Fig. 2), and since it is centered near $v_{\rm sys}$, this line may be due to disk H I at the local systemic velocity. We suspect that the weaker line at -176 km s^{-1} arises in outflowing gas. We are uncertain about the origin of the weak, redshifted "bump" at $\sim +66$ km s^{-1}, but its position and width suggest that it may have been convolved into the southwest jet spectrum from the radio core profiles (see § 3.1.3.).

CBT found doubly peaked [N II] emission at the northeast and southwest radio jets in NGC 1068 (cf. their Fig. 4). They proposed that this emission comes from ionized clouds entrained in a wide (opening angle $\sim 80°$), biconal, nuclear-driven outflow aligned with the radio jets. For this geometry, one can observe only blueshifted outflow gas in radio absorption lines, since the redshifted gas would be located on the far side of the radio source. The blueshifted H I absorption line at the southwest jet may therefore arise in neutral gas participating in the outflow. Since no H I absorption is detected at the northeast radio jet, the entrained clouds probably originate in the inner disk. In addition, there is a region of enhanced column density at the southwest end (i.e., downstream) of the southwest jet (Fig. 3). This enhancement suggests that outflow along the jet axis may have swept up or compressed disk material downstream. The biconal geometry proposed by CBT predicts such a jet/disk interaction: in their model the near edge of the southwest cone is nearly aligned with the inner disk.

3.1.3. *Absorption against the Slightly Resolved Radio Core*

Broad (FWHM $= 128 \pm 25$ km s^{-1}), double absorption lines are present over the southern half of the slightly resolved central radio core. The velocity centers determined from Gaussian fits to the line profiles are $+66 \pm 12$ and -295 ± 9 km s^{-1} relative to $v_{\rm sys}$. These lines are too broad to arise in disk H I (Dickey 1986). Since this profile is unique to the radio core, these lines may instead arise in near-nuclear clouds. The average of the velocity centers of these lines is offset from systemic by -181 km s^{-1}, and it is therefore unlikely that these clouds are in circular orbits in the galactic potential. Since redshifted absorption is present at the radio core, we can rule out the biconal outflow geometry proposed by CBT, and on the basis of the detection of blueshifted absorption we can also rule out strict infall to the radio core. This profile may result instead from two distinct cloud populations: (1) redshifted gas which is falling into the radio core and (2) blueshifted gas which is flowing out of the radio core. These absorption features may therefore be associated with the fueling of and exhaust from the central engine. Higher resolution observations should help resolve these components and constrain the geometry of any radial flow.

3.2. H I *Absorption in NGC 3079*

NGC 3079 is an edge-on galaxy which is host to a massive galactic "superwind" (cf. Duric et al. 1983; Ford et al. 1986; Heckman, Armus, & Miley 1990). The nucleus of NGC 3079 contains subarcsecond, linear radio structure (Irwin & Sequist 1988), and it has been proposed that the superwind is powered either by a corresponding AGN (Filippenko & Sargent 1992) or a nuclear starburst (Heckman et al. 1990). We adopt $v_{\rm sys} =$ 1116 km s^{-1} for NGC 3079 (Irwin & Seaquist 1991). For $H_0 = 50$ km s^{-1} Mpc^{-1}, the distance is 22.3 Mpc, which translates to a scale of 108 pc arcsec^{-1}.

Irwin & Seaquist (1991) have detected spatially unresolved absorption against the radio core in NGC 3079, and our observations partially resolve this absorption. The continuum-weighted optical depth spectrum is given in Figure 4 (*middle panel*). We distinguish two principal components of this spectrum: (1) a broad, central absorption feature (FWZI $\gtrsim 895$ km s^{-1}) with a deep core near the systemic velocity and (2) red- and blueshifted components blended with the broad wings of the central component. We performed a four-component Gaussian decomposition of the average spectrum; the results are also displayed in Figure 4.

We fitted the central absorption feature with two Gaussians: one each for the broad wings and narrower core. The line widths (FWHM) of the fitted Gaussians are (323 ± 13, 84 ± 8) km s^{-1} for the (broad wings, narrow core), and the velocity centers are (1068 ± 4, 1095 ± 2) km s^{-1}. Although the narrow core is centered near $v_{\rm sys}$, it is too broad to originate only in gas far from the radio nucleus (i.e., in the galactic disk), since such gas would be moving tangentially to the line of sight. The

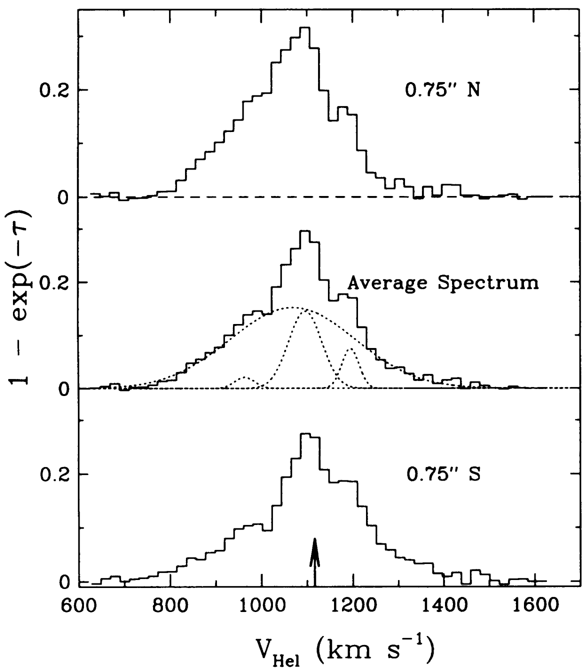

FIG. 4.—Continuum-weighted optical depth spectra extracted for NGC 3079. The systemic velocity (1116 km s^{-1}) is indicated by a vertical arrow. The middle spectrum was extracted from a 3″.5 square region centered on the radio continuum peak. The results of a four-component Gaussian fit are indicated by dotted lines. The top and bottom spectra were extracted from 3″ × 0″.5 strips centered 0″.75 north and 0″.75 south of the radio core, respectively.

broad shape of the central feature may result instead from clouds in rapid orbits near the radio core of the galaxy, with disk H I contributing to the optical depth near v_{sys}. We note also that the central component has a slight blue asymmetry which is apparent both on the extracted spectra and in the velocity difference between the fits to the narrow core and the broad wings. This blue asymmetry suggests the presence of an outflow blended with the rotation. The galactic superwind or the subarcsecond radio jet might power such an outflow.

The blended, Doppler-shifted absorption lines are centered at $+99 \pm 3$ and -132 ± 8 km s^{-1} relative to the narrow core of the central feature. The widths (FWHM) of these lines are 40 ± 6 and 48 ± 28 km s^{-1}, respectively. As illustrated in Figure 4, the blueshifted feature is stronger (weaker) than the redshifted feature 0″.75 north (south) of the radio core. These Doppler-shifted features might arise in a slightly resolved, rotating ring encircling the radio core. The orientation and sense of rotation of these lines are consistent with the large-scale H I emission (Irwin & Seaquist 1991). Assuming that the inner diameter of the ring is ~1″.5 [~170(H_0/50) pc] and that the ring material follows circular orbits, the implied mass interior to the ring is $\sim 3 \times 10^8$ [(H_0/50) sin i]$^{-1}$ $M_\odot$, where i is the inclination of the ring.

4. SUMMARY

The preliminary results for NGC 1068 and NGC 3079 presented here have demonstrated the power of high-resolution H I absorption observations of AGNs. In NGC 1068, we have determined unambiguously the orientation of the linear radio structure, namely, that the northeast lobe is pointed toward us. We have found supportive evidence for an AGN-driven outflow at the southwest jet. There is also an east-west kinematic disturbance in the inner disk suggesting a bar-driven shock in the cold gas. In NGC 3079 the absorption profile is too broad to be explained solely by disk gas, and rapidly moving clouds located near the radio source must contribute to the profile wings. Slightly resolved, blue- and redshifted absorption lines may be due to a ring of cold gas with an inner radius of ~90(H_0/50)$^{-1}$ pc. The mass interior to this postulated ring is $\gtrsim 10^8$ $M_\odot$, implying an extremely dense stellar core or a compact central object.

We wish to thank John Dickey for providing us with a copy of his optical depth spectrum extraction code. We are grateful to Jacqueline van Gorkom, Julian Krolik, and Andrew Wilson for comments which improved the text. This research has made use of the NASA/IPAC Extragalactic Database (NED), which is operated by the Jet Propulsion Laboratory, CalTech, under contract with the National Aeronautics and Space Administration. J. F. G. acknowledges support from an AURA Research Assistantship at STScI.

REFERENCES

Antonucci, R. R. J., & Miller, J. S. 1985, ApJ, 297, 476
Athanassoula, E. 1992a, MNRAS, 259, 328
———. 1992b, MNRAS, 259 345
Bland-Hawthorn, J., Sokolowski, J., & Cecil, G. 1991, ApJ, 375, 78
Brinks, E., Skillman, E. D., Terlevich, R. J., & Terlevich, E. 1994, in preparation
Cecil, G., Bland, J., & Tully, R. B. 1990, ApJ, 355, 70 (CBT)
Dickey, J. 1986, ApJ, 300, 202
Dickey, J., Brinks, E., & Puche, D. 1992, ApJ, 385, 501
Duric, N., Seaquist, E. R., Crane, P. C., Bignell, R. C., & Davis, L. E. 1983, ApJ, 273, L11
Evans, I. N., Ford, H. C., Kinney, A. L., Antonucci, R. R. J., Armus, L., & Caganoff, S. 1991, ApJ, 369, L27
Filippenko, A. V., & Sargent, W. L. W. 1992, AJ, 103, 28
Ford, H., Dahari, O., Jacoby, G., Crane, P. C., & Ciardullo, R. 1986, ApJ, 311, L7
Gallimore, J. F., et al. 1994, in preparation
Heckman, T. M., Armus, L., & Miley, G. K. 1990, ApJS, 74, 833
Heckman, T. M., Balick, B., & Sullivan, W. T. 1978, ApJ, 224, 745
Hodge, P. W. 1968, AJ, 73, 846
Irwin, J. A., & Seaquist, E. R. 1988, ApJ, 335, 658
———. 1991, ApJ, 371, 111
Kaneko, N., Morita, K., Fukui, Y., Sugitani, K., Iwata, T., Nakai, N., Kaifu, N., & Liszt, H. S. 1989, ApJ, 337, 691
Kaneko, N., Morita, K., Fukui, Y., Takahashi, N., Sugitani, K., Nakai, N., & Morita, K.-I. 1992a, PASJ, 44, 341
Kaneko, N., Satoh, T., Kiyotaka, T., Minoru, S., Nichimura, M., & Yamamoto, M. 1992b, AJ, 103, 422
Planesas, P., Scoville, N., & Myers, S. T. 1991, ApJ, 369, 364
Pogge, R. W. 1988 328, 519
Sandage, A. 1961, The Hubble Atlas of Galaxies (Washington, DC: Carnegie Inst. Washington)
Thronson, H. A., et al. 1989, ApJ, 343, 158
Ulvestad, J. S., Neff, S. G., & Wilson, A. S. 1987, AJ, 93, 22
Unger, S. W., Lewis, J. R., Pedlar, A., & Axon, D. J. 1992, MNRAS, 258, 371
Wilson, A. S., & Ulvestad, J. S. 1987, ApJ, 319, 105